Physica B 176 (1992) 180–188
North-Holland

PHYSICA B

# A generalized Dirac–Kronig–Penney model with nonlocal separable potentials

F. Domínguez-Adame and M.A. González
*Departamento de Física de Materiales, Facultad de Ciencias Físicas, Universidad Complutense, 28040-Madrid, Spain*

Received 19 April 1991
Revised manuscript received 18 July 1991

The dispersion relation for relativistic electrons in one-dimensional polyatomic crystals is derived by means of the transfer matrix technique. The interaction of the electron with the lattice is taken to be an array of nonlocal separable potentials arranged periodically. This model leads to exact results even for arbitrary finite-ranged potentials. The $\delta$-function limit is also obtained and the results are compared to results previously found on local $\delta$-function potentials.

## 1. Introduction

The use of the Kronig–Penney model is often restricted to one-dimensional (1D) monatomic crystals (a single atom in the unit cell). Only a few papers [1–4] deal with nonrelativistic electrons in 1D crystals with basis (several atoms in the unit cell). In these papers, the electron interaction with the lattice is taken to be an array of $\delta$-function potentials, arranged periodically. Recently, Domínguez-Adame [5] has provided a generalization of the Kronig–Penney model for relativistic electrons in 1D polyatomic crystals, the so-called generalized Dirac–Kronig–Penney model. The advantage of using $\delta$-function potentials is the existence of exact solutions in both nonrelativistic and relativistic frameworks. Nevertheless, there exist limitations to the use of $\delta$-function potentials to replace actual atomic potentials, as pointed out by Erdös and Herndon [6]. This is easily understood considering that a zero-ranged potential is a crude picture of the electron interaction with atoms in a solid.

The aim of this paper is to present an alternative way to describe the dynamics of relativistic electrons in 1D polyatomic crystals. The reduction to nonrelativistic electrons may be obtained in a similar way. The model is not only exactly solvable but also it is not restricted to zero-ranged potentials. The starting point is the possibility of finding a nonlocal separable potential, or a sum of nonlocal separable potentials, which can reproduce any set of given atomic states [7, 8]. In one dimension, a single-site nonlocal separable potential is constructed as

$$V\psi = \lambda v(x) \int_{-\infty}^{\infty} \mathrm{d}x'\, v(x')\psi(x')\,, \tag{1}$$

where $\lambda$ is the coupling constant and $v(x)$ is a shape function of finite range. The Dirac equation is exactly solvable for such a potential in a rather simple way [9], without requiring the $\delta$-function limit of $v(x)$. A periodic chain of potentials of the form (1) has been considered by Glasser [10] to study the dynamics of Dirac particles in 1D monatomic crystals. The dispersion relation has been found by solving a $2 \times 2$ determinant. The treatment given by Glasser may be applied to polyatomic crystals with

0921-4526/92/$05.00 © 1992 – Elsevier Science Publishers B.V. All rights reserved

$M$ different atoms in the unit cell, but in this case the dispersion relation is calculated through a $2M \times 2M$ determinant. To avoid this difficulty we have found it most appropriate to use the transfer matrix method to solve the 1D Dirac equation ($\hbar = c = 1$)

$$(\sigma_x p + \sigma_z m - E)\psi = -V\psi \,, \tag{2}$$

where the nonlocal potential is assumed to be

$$V\psi = \sum_{n=-\infty}^{\infty} \sum_{\mu=1}^{M} \lambda_\mu v(x - x_\mu - nL) \int_{-\infty}^{\infty} \mathrm{d}x'\, v(x' - x_\mu - nL)\psi(x') \,, \tag{3}$$

in the position representation. Here $\sigma$ denotes the usual Pauli matrix acting upon the two-component wave function $\psi$. Each atom is placed at the position $x_\mu$ ($x_0 = 0 < x_1 < x_2 \cdots < x_M < x_{M+1} = L$) of the unit cell $[0, L]$. Note that we have taken the same shape function $v(x)$ for all the atoms, although different shape functions could also be considered. We shall deal with even $v(x)$ functions. For simplicity we suppose that $v(x)$ vanishes beyond some finite distance $a$ (the exact value of $a$ is not a crucial parameter of the model) and that $\min|x_\mu - x_{\mu-1}| > 2a$ (nonoverlapping potentials). These assumptions are not too restrictive to simulate actual crystal potentials because electrons behave as nearly free particles in the region between atoms [11].

## 2. Transfer matrix for the single-site potential

Firstly, we calculate the transfer matrix for the Dirac equation (2) with a single-site potential (1). The solution of the equation

$$(\sigma_x p + \sigma_z m - E)\psi(x) = -\lambda v(x) \int_{-\infty}^{\infty} \mathrm{d}x'\, v(x')\psi(x') \tag{4}$$

may be written as

$$\psi(x) = A_+ \begin{pmatrix} 1 \\ \xi^{-1} \end{pmatrix} \mathrm{e}^{\mathrm{i}qx} + A_- \begin{pmatrix} 1 \\ -\xi^{-1} \end{pmatrix} \mathrm{e}^{-\mathrm{i}qx} - \lambda \int_{-\infty}^{\infty} \mathrm{d}x'\, G(x, x'; E) v(x') \chi \,, \tag{5}$$

where $q = (E^2 - m^2)^{1/2}$, $\xi = [(E + m)/(E - m)]^{1/2}$, $A_\pm$ are constants, and

$$\chi = \begin{pmatrix} \chi_1 \\ \chi_2 \end{pmatrix} = \int_{-\infty}^{\infty} \mathrm{d}x\, v(x)\psi(x) \,. \tag{6}$$

The Green function for $E^2 > m^2$ is given by

$$G(x, x'; E) = \frac{\mathrm{i}}{2} \mathrm{e}^{\mathrm{i}q|x - x'|} \begin{pmatrix} \xi & \mathrm{sgn}(x - x') \\ \mathrm{sgn}(x - x') & \xi^{-1} \end{pmatrix} . \tag{7}$$

Inserting (5) in (6) we obtain the following relations

$$A_\pm = \frac{1}{2v(q)} [(1 + \mathrm{i}\lambda J(q)\xi/2)\chi_1 \pm (\xi + \mathrm{i}\lambda J(q)/2)\chi_2] \,, \tag{8}$$

where

$$J(q) = \int_{-\infty}^{\infty} \mathrm{d}x \int_{-\infty}^{\infty} \mathrm{d}x'\, v(x)v(x')\, \mathrm{e}^{\mathrm{i}q|x-x'|}\,, \tag{9a}$$

$$v(q) = \int_{-\infty}^{\infty} \mathrm{d}x\, v(x)\, \mathrm{e}^{\mathrm{i}qx}\,. \tag{9b}$$

We have used that $v(x) = v(-x)$, so double-integrals involving off-diagonal elements of $G(x, x'; E)$ vanish.

On the other hand, the wave function for $|x| > a$ must be a combination of plane waves. From (5) we find

$$\begin{aligned}\psi(x) &= A_+\begin{pmatrix}1\\ \xi^{-1}\end{pmatrix}\mathrm{e}^{\mathrm{i}qx} + \left[A_- - \frac{\mathrm{i}}{2}\,\lambda v(q)(\xi\chi_1 - \xi_2)\right]\begin{pmatrix}1\\ -\xi^{-1}\end{pmatrix}\mathrm{e}^{-\mathrm{i}qx}\,, \quad x < a\\ &= \left[A_+ - \frac{\mathrm{i}}{2}\,\lambda v(q)(\xi\chi_1 + \xi_2)\right]\begin{pmatrix}1\\ \xi^{-1}\end{pmatrix}\mathrm{e}^{\mathrm{i}qx} + A_-\begin{pmatrix}1\\ -\xi^{-1}\end{pmatrix}\mathrm{e}^{-\mathrm{i}qx}\,, \quad x > a\end{aligned} \tag{10}$$

Considering a normalized plane wave incident from the left ($A_+ = 1$, $A_- = 0$), one can calculate the transmission $t$ and reflection $r$ amplitudes. Using (8) the result is

$$t = \frac{1 - \lambda EI(q)/q + \lambda^2(R^2(q) + I^2(q))/4}{1 + \mathrm{i}\lambda EJ(q)/q - \lambda^2 J^2(q)/4}\,, \tag{11a}$$

$$r = \frac{-\mathrm{i}\lambda mR(q)/q}{1 + \mathrm{i}\lambda EJ(q)/q - \lambda^2 J^2(q)/4}\,, \tag{11b}$$

with the notation $R(q) = \mathrm{Re}(J(q))$ and $I(q) = \mathrm{Im}(J(q))$. It is an easy matter to check that the unitarity condition $|t|^2 + |r|^2 = 1$ is fulfilled.

The transfer matrix $R$ for the single-site potential relates the wave function on the right to the wave function on the left. Here $R$ may be written as

$$R = \begin{pmatrix}\alpha & \beta\\ \beta^* & \alpha^*\end{pmatrix}, \tag{12}$$

where $\alpha = 1/t^*$ and $\beta = r/t$ so that $\det(R) = 1$. For a nonlocal separable potential with strength $\lambda_\mu$ and centered at any arbitrary point $x_\mu$, the transfer matrix elements transform according to $\alpha_\mu \to \alpha_\mu$ and $\beta_\mu \to \beta_\mu \exp(-2\mathrm{i}qx_\mu)$. Therefore

$$\alpha_\mu = \frac{1}{D_\mu^+}\,[D_\mu^- - \mathrm{i}\lambda_\mu R(q)(E/q - \lambda_\mu I(q)]\,, \tag{13a}$$

$$\beta_\mu = \frac{-\mathrm{i}}{D_\mu^+}\,[\lambda_\mu mR(q)/q]\exp(-2\mathrm{i}qx_\mu)\,, \tag{13b}$$

where we have defined the real parameters

$$D_\mu^\pm = 1 - \lambda_\mu EI(q)/q + \tfrac{1}{4}\lambda_\mu^2[I^2(q) \pm R^2(q)]\,. \tag{14}$$

## 3. Transfer matrix for the unit cell

The potential in the unit cell,

$$V\psi = \sum_{\mu=1}^{M} \lambda_\mu v(x - x_\mu) \int_{-\infty}^{\infty} \mathrm{d}x'\, v(x' - x_\mu)\psi(x') , \tag{15}$$

is a superposition of non-overlapping single-site potentials. Therefore, the transfer matrix for the unit cell

$$T_M = \begin{pmatrix} A_M & B_M \\ A_M^* & B_M^* \end{pmatrix} \tag{16}$$

may be obtained as a matrix product

$$T_M = R_M R_{M-1} \cdots R_1 , \tag{17}$$

where the matrix elements of each $R_\mu$ are given by (13). Let $T_{M-1}$ be the transfer matrix for the first $M-1$ single-site potentials, i.e. the unit cell except the last atom. Hence we can write

$$T_M = R_M T_{M-1} , \tag{18}$$

and then we find the recurrence relation

$$A_M = (\alpha_M + \alpha_{M-1}^* \beta_M / \beta_{M-1}) A_{M-1} - (\beta_M / \beta_{M-1}) A_{M-2} , \tag{19}$$

with the initial conditions $A_0 = 1$ and $A_1 = \alpha_1$. An analogous equation can be stated for $B_M$. This recurrence relation may be transformed into two coupled recurrence relations for the real and imaginary parts of the $A$s, only involving real coefficients.

## 4. Dispersion relation in polyatomic crystals

The polyatomic crystal we consider is a periodic repetition of the unit cell, so the lattice potential is a periodic array of potentials given by (15). The Bloch theorem provides a link between the values of the electronic wave function at $x = 0$ and $x = L$. This theorem ensures that $\psi(L) = \exp(\mathrm{i}kL)\psi(0)$, where $k$ is the crystal momentum. We have assumed that the electron is nearly free in the vicinity of the unit cell boundaries. Therefore

$$\psi(0) = QM(0)\phi_0 , \tag{20a}$$

$$\psi(L) = QM(L)\phi_L , \tag{20b}$$

where $M(x) = \mathrm{diag}(\mathrm{e}^{\mathrm{i}qx}, \mathrm{e}^{-\mathrm{i}qx})$ and $Q$ is an energy-dependent matrix given by

$$Q = \begin{pmatrix} 1 & 1 \\ \xi^{-1} & -\xi^{-1} \end{pmatrix} , \tag{21}$$

and $\phi_0$, $\phi_L$ are constant spinors satisfying $\phi_L = T_M \phi_0$. Thus we obtain

$$[e^{ikL} M(0) - M(L) T_M] \phi_0 = 0 . \tag{22}$$

Requiring the determinant to vanish for nontrivial solutions one gets

$$\cos kL = \mathrm{Re}(A_M) \cos qL - \mathrm{Im}(A_M) \sin qL . \tag{23}$$

Real and imaginary parts of $A_M$ are recursively calculated from (19). Real values of $k$, obtained by the usual search methods, give us the dispersion relation $E(k)$ and consequently the band structure of the polyatomic crystal.

If only a few atoms are placed in the unit cell of the crystal, the dispersion law (23) can be written in a more simplified form. For monatomic crystals we have $A_1 = \alpha_1$ so that

$$D_1^+ \cos kL = D_1^- \cos qL + \lambda_1 R(q)(E/q - \lambda_1 I(q)/2) \sin qL . \tag{24}$$

For two different atoms in the unit cell $A_2 = \alpha_1 \alpha_2 + \beta_1^* \beta_2$. Hence

$$\begin{aligned} D_1^+ D_2^+ \cos kL = {} & D_1^- D_2^- \cos qL + \lambda_1 \lambda_2 R^2(q)(m^2/q^2 - (E/q - \lambda_1 I(q)/2)(E/q - \lambda_2 I(q)/2)) \cos qL \\ & + R(q)(\lambda_2 D_1^- (E/q - \lambda_1 I(q)/2) + \lambda_1 D_2 (E/q - \lambda_2 I(q)/2)) \sin qL \\ & + 2\lambda_1 \lambda_2 (m^2/q^2) R(q) \sin q(x_2 - x_1) \sin q(L - x_2 + x_1) . \end{aligned} \tag{25}$$

## 5. $\delta$-function limit

In the last sections we consider arbitrary even functions $v(x)$ in (3). To compare our results with that obtained by solving the Dirac equation for the local potential [5]

$$V(x) = \sum_{n=-\infty}^{\infty} \sum_{\mu=1}^{M} \lambda_\mu \delta(x - x_\mu - nL) , \tag{26}$$

we take the limit $v(x) \to \delta(x)$ in the above equations. In such a case, $J(q) = 1$, and then the matrix elements (13) reduce to

$$\alpha_\mu = \cos \theta_\mu - \mathrm{i} \frac{E}{q} \sin \theta_\mu , \tag{27a}$$

$$\beta_\mu = -\mathrm{i} \frac{m}{q} \sin \theta_\mu \exp(-2\mathrm{i} q x_\mu) , \tag{27b}$$

where $\sin \theta_\mu = \lambda_\mu / (1 + \lambda_\mu^2/4)$. For $M = 1$ the dispersion relation is simply written as

$$\cos kL = \cos \theta_1 \cos qL + (E/q) \sin \theta_1 \sin qL , \tag{28}$$

and for $M = 2$ we obtain

$$\begin{aligned} \cos kL = {} & \cos(\theta_1 + \theta_2) \cos qL + (E/q) \sin(\theta_1 + \theta_2) \sin qL \\ & + 2(m/q)^2 \sin \theta_1 \sin \theta_2 \sin q(x_2 - x_1) \sin q(L - x_2 + x_1) . \end{aligned} \tag{29}$$

As we mentioned above, it is instructive to compare our results as $v(x) \to \delta(x)$ with those obtained for the Dirac equation with local $\delta$-function potentials. This problem has been recently solved by Domínguez-Adame [5] using a transfer matrix technique. For single-site potentials of the form $\lambda_\mu \delta(x - x_\mu)$ he has shown that the transfer matrix elements are given by

$$\alpha_\mu = \cos \lambda_\mu - \mathrm{i} \frac{E}{q} \sin \lambda_\mu \,, \tag{30a}$$

$$\beta_\mu = -\mathrm{i} \frac{m}{q} \sin \lambda_\mu \exp(-2\mathrm{i}qx_\mu) \,. \tag{30b}$$

We notice that these matrix elements are different to those given in (27). Both results only agree in the weak coupling limit ($\lambda \ll 1$). This inconsistency comes from the fact that a relativistic, local $\delta$-function potential is not the limiting case of a single nonlocal separable potential, as pointed out by Calkin et al. [12]. Since local $\delta$-function potentials present ambiguities when introduced in the Dirac equation at the outset (ref. [13] and references therein), nonlocal separable potentials are the natural extension to obtain solvable band models. At low energies and weak couplings, both nonlocal and local $\delta$-function potentials yield the same dispersion relation, and the latter coincides with that obtained by solving the Schrödinger equation for the potential (3), reported in refs. [1–4]. In that limit situation the matrix elements (27) and (30) reduce to

$$\alpha_\mu = 1 - \mathrm{i} \frac{m}{q'} \lambda_\mu \,, \tag{31a}$$

$$\beta_\mu = -\mathrm{i} \frac{m}{q'} \lambda_\mu \exp(-2\mathrm{i}q'x_\mu) \,, \tag{31b}$$

where $q' = [2m(E - m)]^{1/2}$, in agreement with the nonrelativistic results of Erdös and Herndon [6]. Let us comment that the Dirac–Kronig–Penney model cannot be generalized to three dimensions using local $\delta$-function potentials [14]. Therefore, nonlocal separable potentials provide a simple way to obtain solvable equations for relativistic band structures in three dimensions.

## 6. Numerical results and discussions

In this section we discuss some numerical results for relativistic particles in both monatomic and diatomic lattices. Results are compared with nonrelativistic predictions. In order to facilitate a direct comparison between nonrelativistic and relativistic energy values, we introduce the parameter $\varepsilon = E - m$ for relativistic particles, whereas $\varepsilon$ will simply denote the energy of nonrelativistic particles. We use units such that $m = 1$ hereafter. For our numerical studies we have chosen the following shape function

$$\begin{aligned} v(x) &= 1/2a \,, \quad |x| < a \,, \\ &= 0 \,, \qquad |x| > a \,. \end{aligned}$$

To avoid the profusion of free parameters we have taken $a = 0.5$. Values of the coupling constants range from 0.01 to 1. Since the single-site potentials are then repulsive for particles (and attractive for antiparticles) we only consider positive values of the parameter $\varepsilon$.

Figure 1 shows the dispersion relation $\varepsilon(k)$ for two different monatomic lattices with period $L = \pi$,

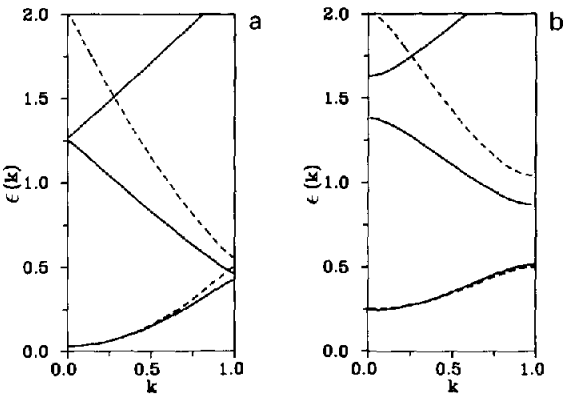


Fig. 1. Dispersion relation for nonrelativistic (dashed lines) and relativistic (solid lines) particles in a monatomic lattice of period $L = \pi$ and coupling constant (a) $\lambda = 0.1$ and (b) $\lambda = 1$.

and $\lambda = 0.1$ and $\lambda = 1$, respectively. We observe that gaps become wider and bandwidths narrower with increasing value of the coupling constant $\lambda$, for both nonrelativistic and relativistic particles. The position of the bottom of the first allowed band is the same in the nonrelativistic and relativistic cases, so the first gap remains unchanged when relativity is considered. Nevertheless, the second gap is narrower for relativistic particles (see fig. 2). This result is in contrast to that obtained by Glasser and Davison [15] in dealing with the Dirac–Kronig–Penney model (a Dirac particle in a periodic array of $\delta$-function potentials), who found that all gaps are not affected by relativity. However, our results are in good agreement to that found by solving the wave equations for more realistic potentials like the Mathieu potential [16]. In this case, the gaps are also narrower for relativistic particles.

We have found that the top of the first allowed band is 0.500 for nonrelativistic particles in monatomic lattices, no matter the value of the coupling constant. On the contrary, this energy gradually increases from 0.415 to 0.650 with increasing $\lambda$ in the case of relativistic particles. The width of the first allowed band is also found to be smaller for relativistic particles, in the case of relatively weak coupling,

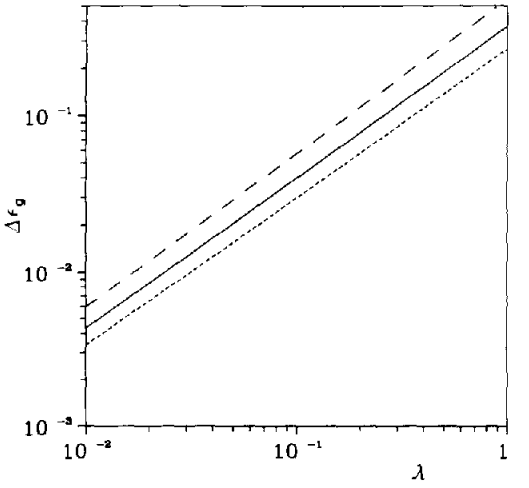


Fig. 2. First gap for nonrelativistic and relativistic particles (short-dashed line) and second gap for nonrelativistic (long-dashed line) and relativistic (solid line) particles in a monatomic lattice of period $L = \pi$, as a function of the coupling constant.

as seen in fig. 3. This *shrinkage* of the spectrum has also been observed in the periodic [15] as well as in the quasiperiodic [17] Dirac–Kronig–Penney models. It can be seen in fig. 3 that the allowed band is wider in the relativistic case for $\lambda$ larger than about 0.8. For large values of the coupling constant, nonrelativistic and relativistic bandwidths show a rather different behaviour. Nonrelativistic bandwidths diminish gradually as $\lambda$ increases, whereas relativistic bandwidths decrease up to a value of $\lambda = 1.5$ and then increase with $\lambda$. This fact may be qualitatively understood considering that an electrostatic-like potential with large, positive coupling constant strongly binds an antiparticle, so mixing of particle and antiparticle states will occur in that case. One cannot expect to observe this phenomenon in ordinary solids because it requires very high values of the coupling constant. However, it would be an appreciable effect in the nuclear model of McKellar and Stephenson [18], in which quarks are assumed to move in a one-dimensional periodic structure.

Relativistic effects in diatomic lattices are rather similar to those discussed above. In particular, the *shrinkage* of the spectrum is observed when relativistic effects are considered, except that the first gap remains unchanged. The first gap as a function of the coupling constant is shown in fig. 4. As expected, the gap increases as $\lambda_1$ and $\lambda_2$ increase.

Concerning the band structure in one-dimensional binary alloys, Saxon and Hutner [19] proposed the following conjecture: "Forbidden energies which are common to a pure A lattice and a pure B lattice (with the same lattice period) will always be forbidden in any arrangement of A and B atoms in a substitutional solid solution". The proof of this conjecture for nonrelativistic electrons in the special case of $\delta$-function potentials was given by Luttinger [20]. Relativistic generalizations of the Saxon–Hutner conjecture has been discussed in refs. [21, 22]. Our numerical results suggest that the relativistic Saxon–Hutner theorem is also valid for nonlocal potentials. In fig. 5 we show the allowed bands of two different monatomic lattices, with period $L = \pi$ and coupling constants $\lambda = 0.3$ and $\lambda = 0.8$, along with the allowed bands of a diatomic lattice with $\lambda_1 = 0.3$ and $\lambda_2 = 0.8$, with a distance between nearest-neighbours $L = \pi$ (period $L = 2\pi$). We notice that the prediction of the Saxon–Hutner theorem is still valid in this case.

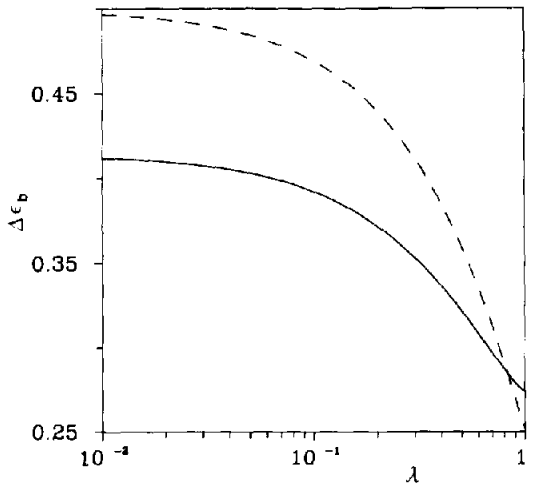


Fig. 3. Width of the first allowed band for nonrelativistic (dashed line) and relativistic (solid line) particles in a monatomic lattice of period $L = \pi$, as a function of the coupling constant.

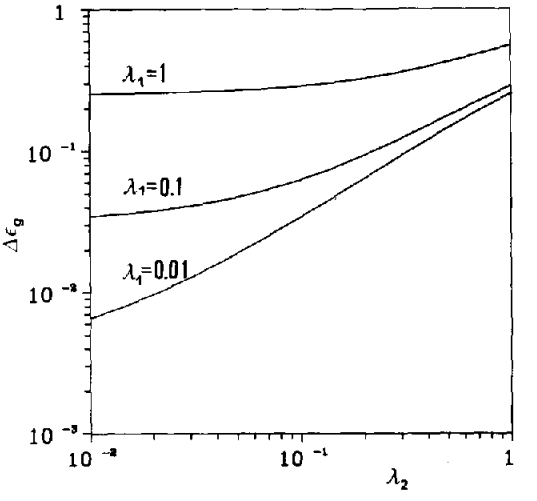


Fig. 4. First gap for nonrelativistic and relativistic particles in a diatomic lattice of period $L = \pi$ and $x_2 - x_1 = 1.1$, as a function of $\lambda_2$ for different values of $\lambda_1$.

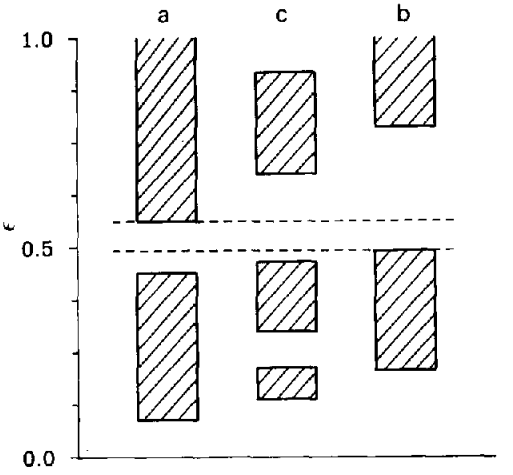


Fig. 5. Comparison between allowed bands (hatched areas) and gaps of monatomic lattices with period $L = \pi$ and coupling constants (a) $\lambda = 0.3$ and (b) $\lambda = 0.8$ with (c) the band structure of a diatomic lattice with period $L = 2\pi$, distance between nearest-neighbours $x_2 - x_1 = \pi$ and coupling constants $\lambda_1 = 0.3$ and $\lambda_2 = 0.8$. Dashed lines indicate common forbidden energies.

## Acknowledgement

The authors thank Dr. C.L. Roy for helpful comments.

## References

[1] C.L. Roy and K. Bhattacharya, Indian J. Pur. Appl. Phys. 7 (1969) 306.
[2] P.H.A. Santana and A. Rosato, Am. J. Phys. 41 (1973) 1138.
[3] A.M. Eldib, H.F. Hassan and M.A. Mohamed, J. Phys. C 20 (1987) 3011.
[4] V.M. Gasparian, B.L. Altshuler, A.G. Aronov and Z.A. Kasamanian, Phys. Lett. A 132 (1988) 201.
[5] F. Dominguez-Adame, J. Phys. Condens. Mat. 1 (1989) 109.
[6] P. Erdös and R.C. Herndon, Helv. Phys. Acta 50 (1977) 513.
[7] B.W. Knight and G.A. Peterson, Phys. Rev. 132 (1963) 1085.
[8] M.L. Glasser, Surf. Sci. 64 (1977) 141.
[9] M.G. Calkin, D. Kiang and Y. Nogami, Phys. Rev. C 38 (1988) 1076.
[10] M.L. Glasser, Am. J. Phys. 51 (1983) 936.
[11] O. Madelung, Introduction to Solid State Theory (Springer, New York, 1987) p. 91.
[12] M.G. Calkin, D. Kiang and Y. Nogami, Am. J. Phys. 55 (1987) 737.
[13] F. Domínguez-Adame and E. Maciá, J. Phys. A 22 (1989) L419.
[14] F. Domínguez-Adame, J. Phys. A 22 (1990) 1993.
[15] M.L. Glasser and S.G. Davison, Int. J. Quantum Chem. IIIS (1970) 867.
[16] B. Méndez and F. Domínguez-Adame, J. Phys. A 24 (1991) L331.
[17] F. Domínguez-Adame and A. Sánchez, Phys. Lett. A 159 (1991) 153.
[18] B.H.J. McKellar and G.J. Stephenson, Phys. Rev. C 35 (1987) 2262.
[19] D.S. Saxon and R.A. Hutner, Philips Res. Rep. 4 (1949) 81.
[20] J.M. Luttinger, Philips Res. Rep. 6 (1951) 303.
[21] B. Subramanian and K.V. Bhagwat, Phys. Stat. Sol. (b) 48 (1971) 399.
[22] I.M. Mladenov, Phys. Lett. A 137 (1989) 313.